Measurement of the Higgs boson production in decays of two τ leptons using the ATLAS detector

Zinonas Zinonos

Max-Planck-Institut für Physik, München

on behalf of the ATLAS collaboration

ATLAS EXPERIMENT

ICHEP Seoul 2018

Max-Planck-Institut für Physik
(Werner-Heisenberg-Institut)

Preamble

Probe the Higgs Yukawa coupling to τ leptons, event frequency and verify the Higgs boson's affinity to mass!

$$\mathcal{L}_{\mathcal{H}} = \left| \left(i\partial_\mu - g\tfrac{1}{2}\boldsymbol{\tau}\cdot\mathbf{W}_\mu - g'\frac{Y}{2}B_\mu \right)\phi \right|^2 - V(\phi) - \left(G_\ell \bar{L}\phi R + \text{h.c.}\right) - \left(G_q \bar{L}\phi_c R + \text{h.c.}\right)$$

$$-m_\tau \tau^+\tau^- - \underbrace{\frac{m_\tau}{v}}_{G_\ell/\sqrt{2}} \tau^+\tau^- h$$

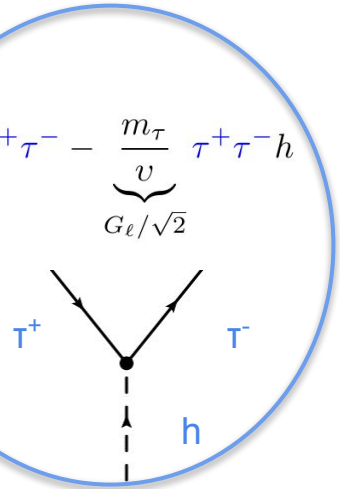

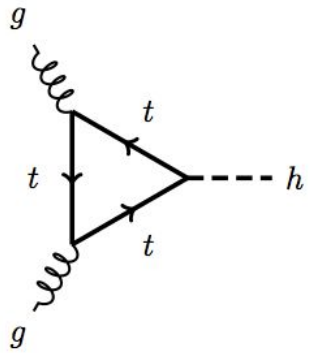

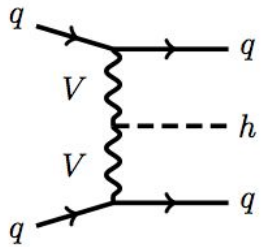

Exploit the 2015+2016 LHC *pp* dataset at $\sqrt{s}$=*13 TeV* (36 fb^{-1}) and combine to previous results $\sqrt{s}$=*7, 8 TeV* (25 fb^{-1}).

H→ττ @ 125 GeV - Retrospect at LHC

Date	Experiment	Result	Significance Obs. (Exp.) [σ]	Reference
May 2014	CMS	evidence	3.2 (3.7)	JHEP05(2014)104
April 2015	ATLAS	evidence	4.5 (3.4)	JHEP04(2015)117
August 2016	ATLAS+CMS	observation	5.5 (5.0)	JHEP08(2016)045
April 2018	CMS	observation	5.9 (5.9)	Phys.Lett. B779 (2018) 283-316
June 2018	ATLAS	observation	6.4 (5.4)	ATLAS-CONF-2018-021

Regions

13 signal regions meticulously designed to exploit signal-sensitive event topologies

- VBF loose, tight defined by m_{jj}, $\Delta\eta_{jj}$, $p_T^{\tau\tau}$
- VBF high-$p_T^{\tau\tau}$
- Boosted high-, low-$p_T^{\tau\tau}$

6 control regions defined to constrain the normalization of the backgrounds in regions where their purity is high (Zll, top).

Expected signal and background composition shown.

→ Important backgrounds: Zττ, jet-faking-τ, Zll, top.

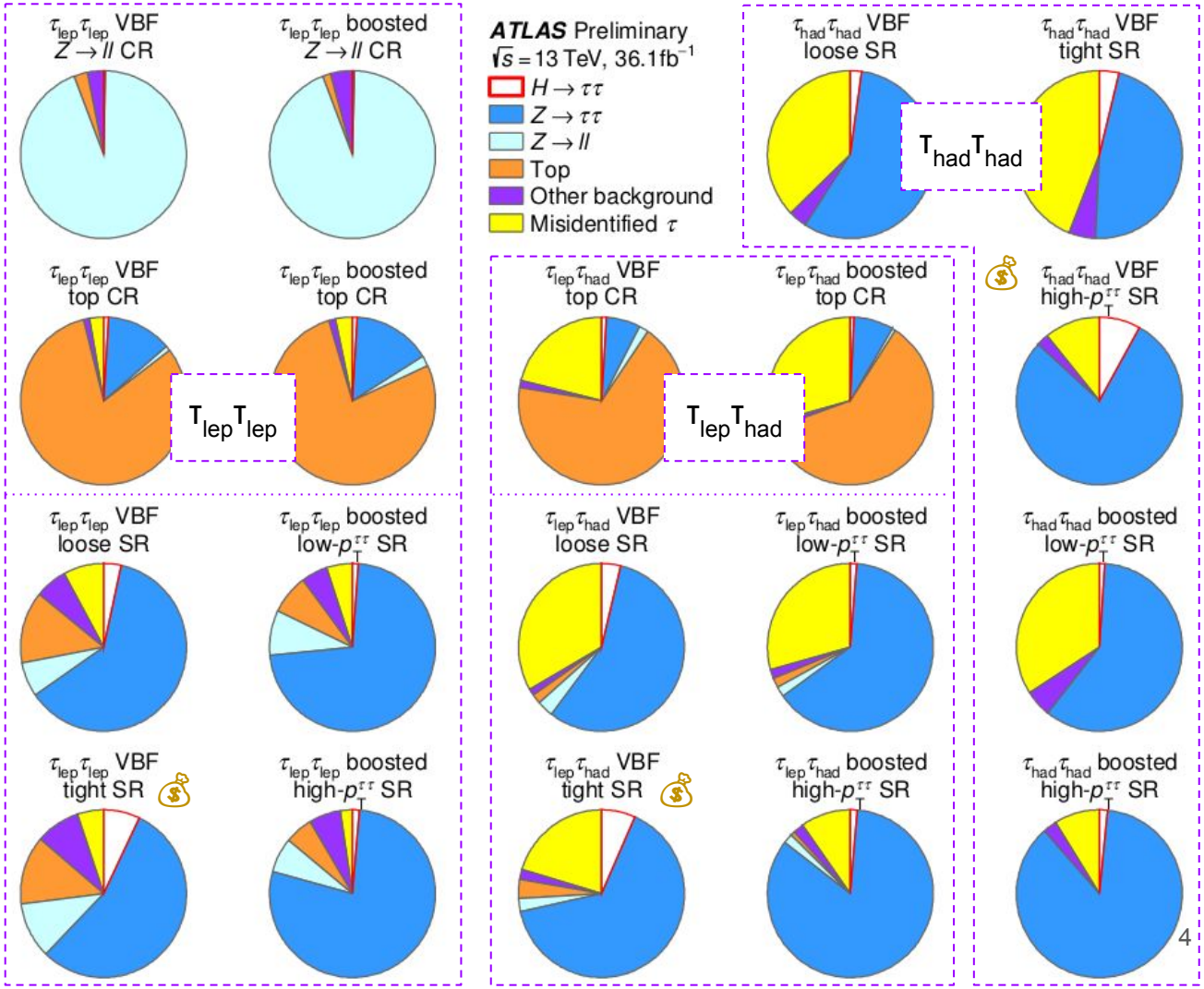

Background Estimate Validation

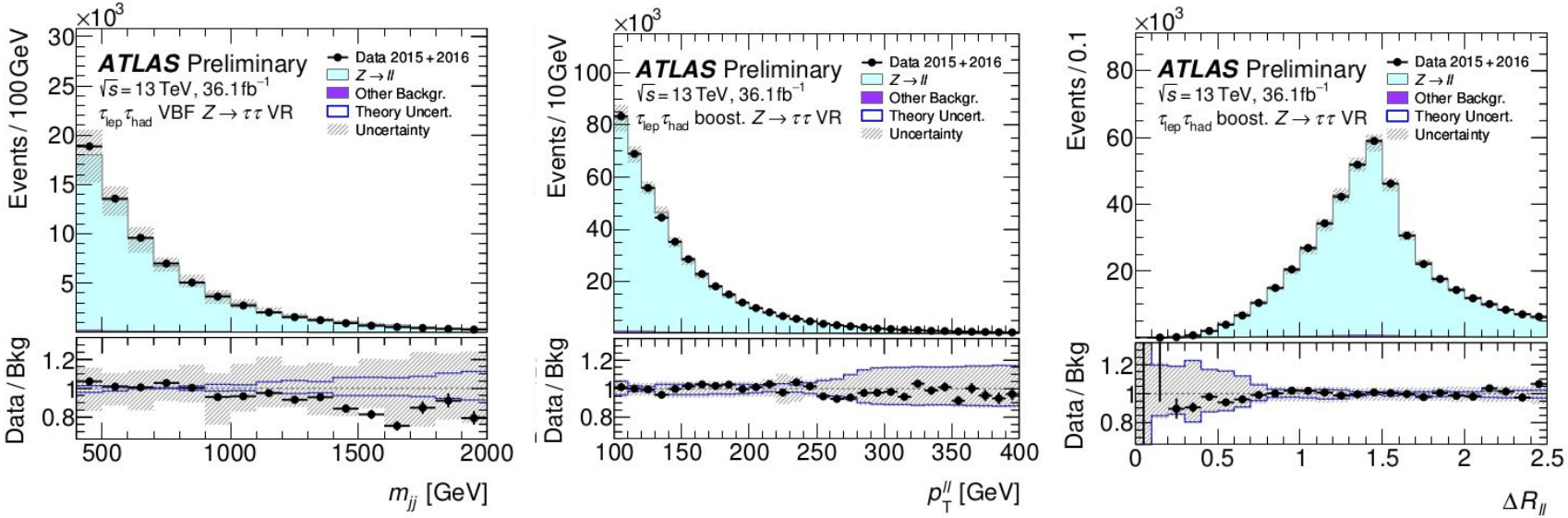

Validation of the dominant, irreducible background DY process $Z/\gamma^* \rightarrow \tau\tau$ is very important:

- Prediction taken from MC (embedding technique in analysis at $\sqrt{s}$=7, 8 TeV).
- Accounts for 50-90% of the total background depending on the SR.
- Separation between the DY and $H \rightarrow \tau\tau$ signal processes is limited by the $m_{\tau\tau}$ reconstruction.
- $Z \rightarrow \tau\tau$ background normalization factor (NF) correlated across channels and constrained by $m_{\tau\tau}$ at Z peak (different NF parametrization for VBF and Boosted).

Background Estimate Validation

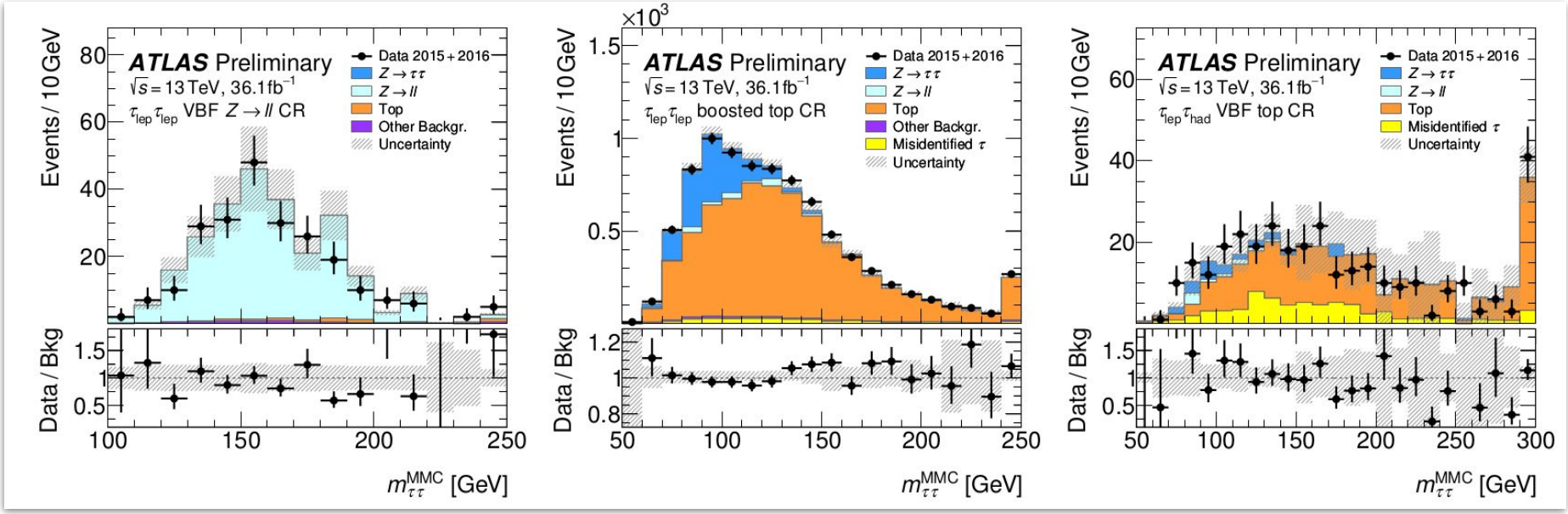

Zll CR $\tau_{lep}\tau_{lep}$ | Top CR $\tau_{lep}\tau_{lep}$ | Top CR $\tau_{lep}\tau_{had}$

$\tau_{lep}\tau_{lep}$ / $\tau_{lep}\tau_{had}$: Background estimate of $Z/\gamma^{*}\rightarrow ll$ and $t\bar{t}/t$ relies on MC but CRs are accommodated to control overall rate and check modeling of most important kinematics

→ Observed event yields in CRs constrain the normalization of respective simulated events in SRs.

Background Estimate Validation

Wjets CR $\tau_{lep}\tau_{had}$

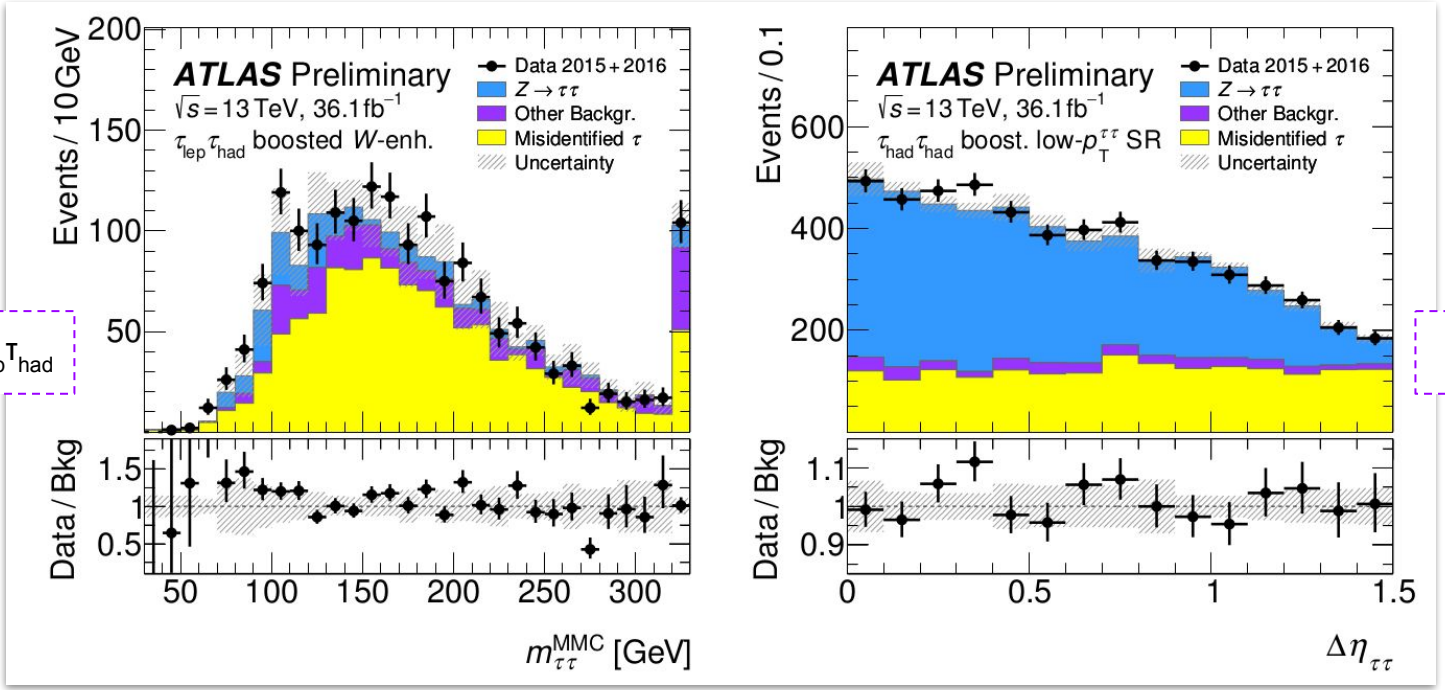

low-$p_T^{\tau\tau}$ $\tau_{had}\tau_{had}$

- **$\tau_{lep}\tau_{had}$:** Data-driven "fake-factor" *F=N(pass ID τ_{had})/N(fail ID τ_{had})* to estimate fake τ_{had} contributions from QCD multijets and W+jets.
- **$\tau_{had}\tau_{had}$:** QCD multijets background modeled using a template extracted from data with τ_{had} candidates of relaxed N(track) requirement and inverted charge-conjugation (free floating NF for fakes in the fit)

Statistical Interpretation

Fit model consisted of 13 SRs and 6 CRs.

m_{MMC} used as observable in the fit.

A maximum likelihood fit is performed on data to extract the parameter of interest

$$\sigma_{H\to\tau\tau} \equiv \sigma_H \cdot \mathcal{B}(H \to \tau\tau)$$

Systematic uncertainties accounted as nuisance parameters in the combined fit.

$$\mu_{H\to\tau\tau} = 1.09\,^{+0.18}_{-0.17}\,(\text{stat.})\,^{+0.27}_{-0.22}\,(\text{syst.})\,^{+0.16}_{-0.11}\,(\text{theory syst.})$$

$$\sigma_{H\to\tau\tau} = 3.71 \pm 0.59\,(\text{stat.})\,^{+0.87}_{-0.74}\,(\text{syst.})\,\text{pb}$$

Vs.

$$\sigma^{\text{SM}}_{H\to\tau\tau} = 3.43 \pm 0.13\,\text{pb}$$

Experimental uncertainties are fully correlated across categories, background modeling uncertainties & NFs are kept uncorrelated (except the Z NF).

Significance of the signal excess with m_H=125 GeV with respect to the SM-background-only hypothesis

√s (TeV)	7, 8	13	Combined
Observed (σ)	4.5	4.4	**6.4**
Expected (σ)	3.4	4.1	5.4

Post-fit plots

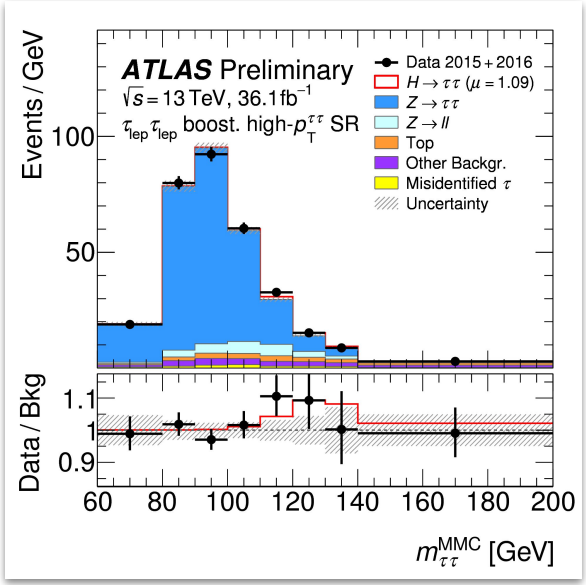

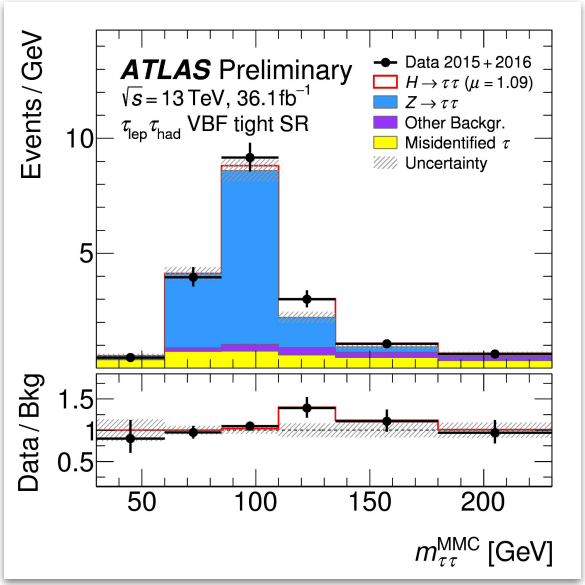

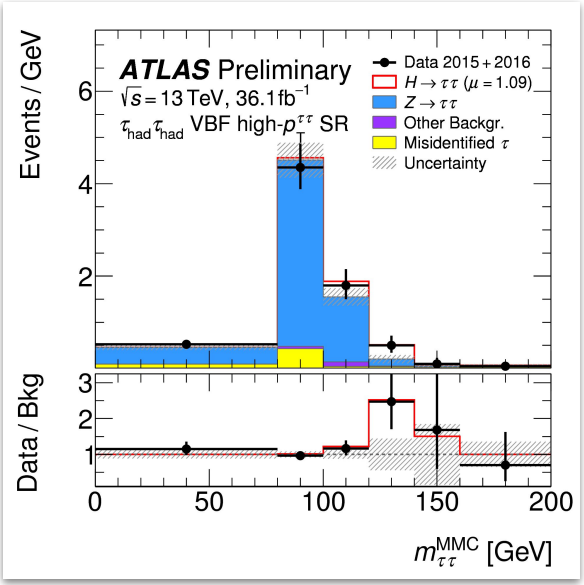

$\tau_{lep}\tau_{lep}$ Boosted

$\tau_{lep}\tau_{had}$ VBF

$\tau_{had}\tau_{had}$ VBF

→Mass estimator distributions

The significant deviation from unity in Data/Bkg around m=125 GeV indicates the presence of the Higgs boson.

Cross Section

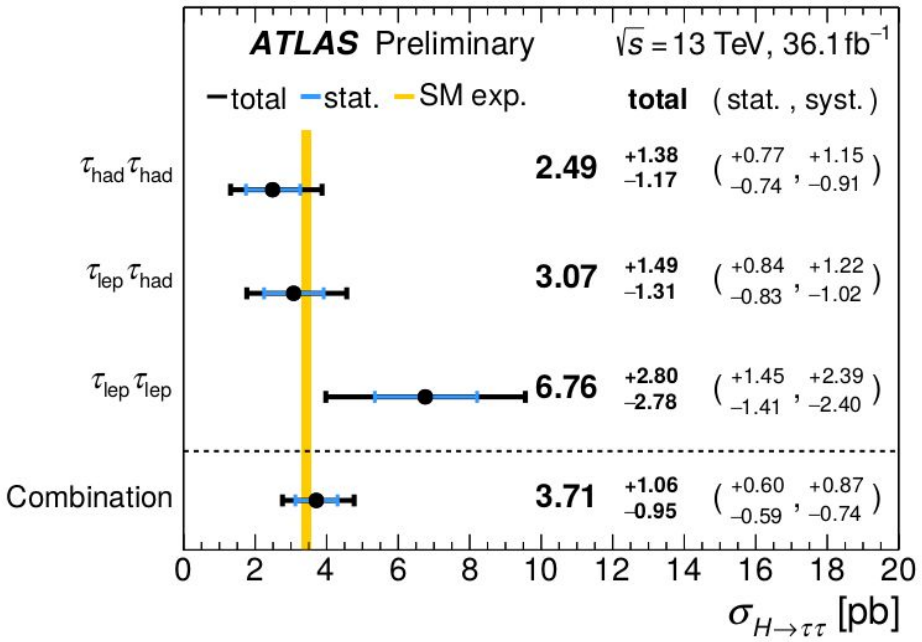

Individual channels

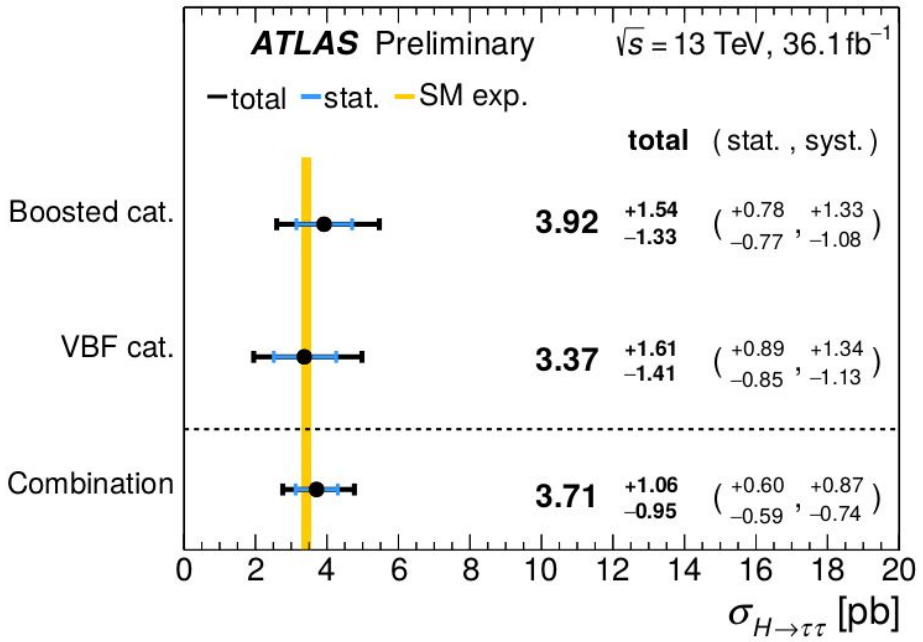

Signal categories

→ VBF and boosted categories provide good sensitivity to VBF and ggF Higgs production.

→ Results are consistent with SM predictions.

Cross Section

Likelihood contours for the combination of all channels as a result of a two-cross-section-parameter fit.

Separate the vector-boson-mediated VBF process from the fermion-mediated ggF process.

→ Strongly anticorrelated results (ρ=-52%).

→ Measurements are consistent with SM predictions.

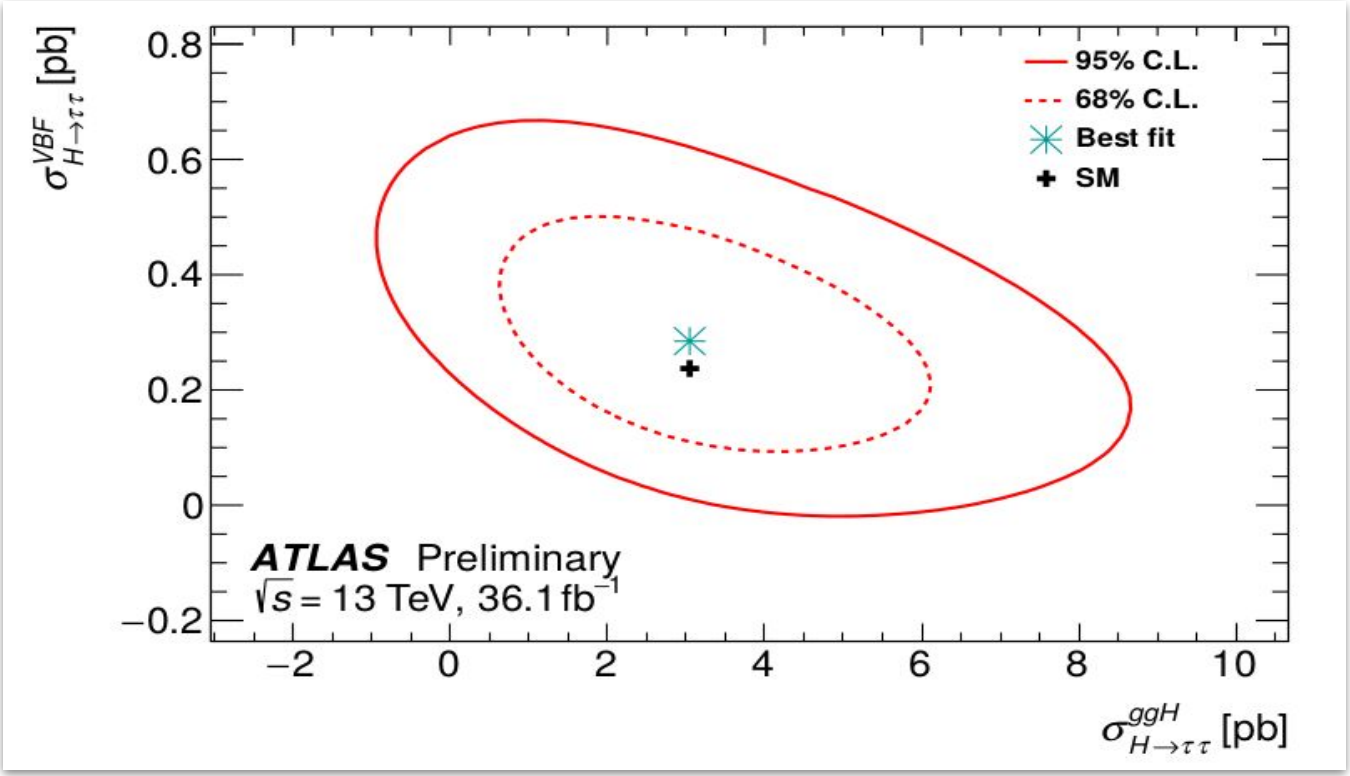

$$\sigma^{\text{VBF}}_{H\to\tau\tau} = 0.28 \pm 0.09\,(\text{stat.})\,^{+0.11}_{-0.09}\,(\text{syst.})\,\text{pb}$$

$$\sigma^{ggF}_{H\to\tau\tau} = 3.0 \pm 1.0\,(\text{stat.})\,^{+1.6}_{-1.2}\,(\text{syst.})\,\text{pb}$$

Vs.

$$\sigma^{\text{SM}}_{\text{VBF},\,H\to\tau\tau} = 0.237 \pm 0.006\,\text{pb}$$

$$\sigma^{\text{SM}}_{ggF,\,H\to\tau\tau} = 3.05 \pm 0.13\,\text{pb}$$

Impact of Systematic Uncertainties

Source of uncertainty	Impact $\Delta\sigma/\sigma_{H\to\tau\tau}$ (%) Observed	Expected
Theoretical uncert. on signal	+13.5 / −8.7	+11.9 / −7.7
Background statistics	+11 / −10	+10.2 / −9.8
Jets and $E_{\mathrm{T}}^{\mathrm{miss}}$	+11.5 / −9.3	+10.5 / −8.6
Background normalization	+6.8 / −4.8	+6.6 / −4.6
Misidentified τ	+4.5 / −4.2	+3.7 / −3.4
Theoretical uncert. on background	+4.6 / −3.6	+5.1 / −4.2
Hadronic taus	+4.7 / −3.0	+5.8 / −4.2
Flavour tagging	+3.3 / −2.4	+2.9 / −2.2
Luminosity	+3.3 / −2.3	+3.1 / −2.2
Electrons and muons	+1.2 / −1.0	+1.1 / −0.9
Total systematic uncert.	+24 / −20	+22 / −19
Data statistics	±16	±15
Total	+28 / −26	+27 / −25

Ranked, fractional impact of systematic uncertainties in $\sigma_{H\to\tau\tau}$ as computed by the fit.

"Background statistics" is dominated by the low MC statistics available for the Z+jets MC sample in the SR phase space.

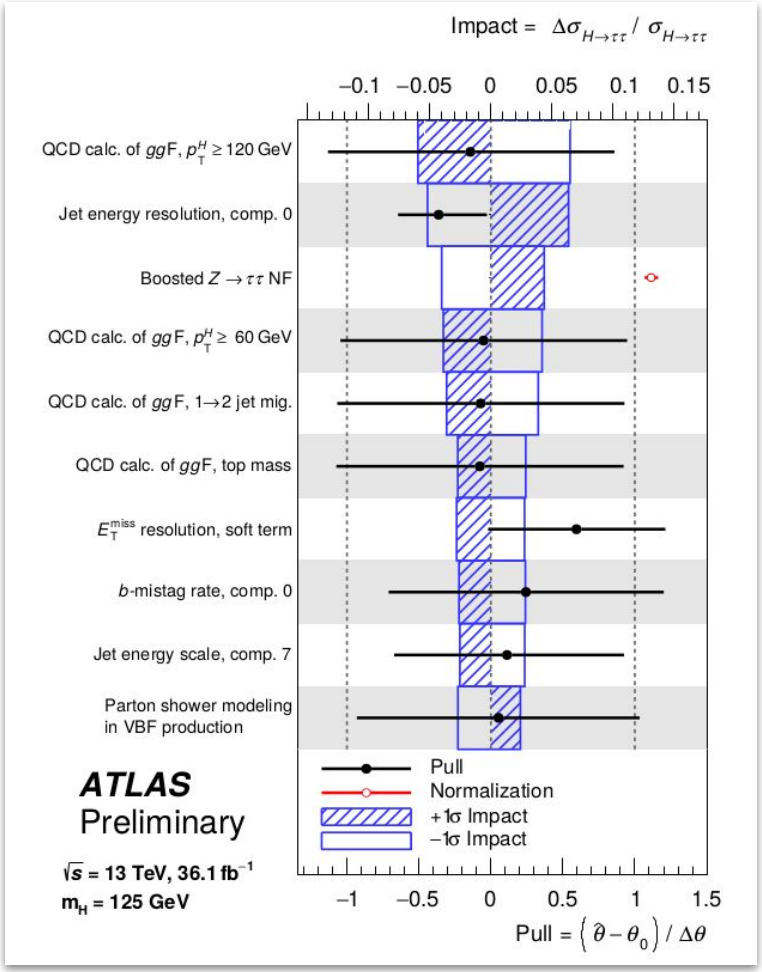

Synopsis

- ATLAS firmly establishes an observation of the Higgs boson coupling to the heaviest lepton of SM and thus the mass generation mechanism for leptons.
- Releases also a H→ττ total production cross section measurement of 3.7 pb with a relative uncertainty of 28%; well in agreement with the SM prediction, but leaves also room for new physics contributions to be unveiled with more data.
- The result, in addition, disentangles the two most common Higgs production mechanisms: gluon-gluon fusion and weak boson fusion.
- Bright prospects ahead as the recent result from ATLAS lays the ground for studying Higgs to τ-pair decays in detail.
- Scrutinizing the tiny details of the H→ττ properties may open a new window to search for signs of new physics.
- With the much larger dataset available at the end of LHC Run 2, these details can now be studied in-depth.

Auxiliary Material

Data and simulated samples

Process	Monte Carlo generator	PDF	UEPS	Cross-section order
ggF	POWHEG-BOX v2	PDF4LHC15 NNLO	PYTHIA 8.212	N^{3}LO QCD + NLO EW
VBF	POWHEG-BOX v2	PDF4LHC15 NLO	PYTHIA 8.212	~NNLO QCD + NLO EW
VH	POWHEG-BOX v2	PDF4LHC15 NLO	PYTHIA 8.212	NNLO QCD + NLO EW
W/Z + jets	SHERPA 2.2.1	NNPDF30NNLO	SHERPA 2.2.1	NNLO
$VV/V\gamma^*$	SHERPA 2.2.1	NNPDF30NNLO	SHERPA 2.2.1	NLO
$t\bar{t}$	POWHEG-BOX v2	CT10	PYTHIA 6.428	NNLO+NNLL
Wt	POWHEG-BOX v1	CT10F4	PYTHIA 6.428	NLO

The overall normalization of the ggF process is taken from a next-to-next-to-next-to-leading-order (N^{3}LO) QCD calculation with NLO EW corrections applied.

Production by VBF is normalized to an approximate-NNLO QCD cross section with NLO EW corrections applied.

The VH samples are normalized to cross sections calculated at NNLO in QCD, with NLO EW radiative corrections applied.

Triggers

Analysis channel	Trigger	Analysis p_T requirement [GeV] 2015	2016
$\tau_{lep}\tau_{lep}$ & $\tau_{lep}\tau_{had}$	Single electron	25	27
	Single muon	21	27
$\tau_{lep}\tau_{lep}$	Di-electron	15 / 15	18 / 18
	Di-muon	19 / 10	24 / 10
	Electron+muon	18 / 15	18 / 15
$\tau_{had}\tau_{had}$	Di-$\tau_{had\text{-}vis}$	40 / 30	40 / 30

Electrons: medium ID, gradient isolation

Muons: medium ID, gradient isolation

Taus: medium BDT, 1- or 3-prongs

Event selection

$\tau_{\text{lep}}\tau_{\text{lep}}$		$\tau_{\text{lep}}\tau_{\text{had}}$	$\tau_{\text{had}}\tau_{\text{had}}$
$ee/\mu\mu$	$e\mu$		
$N_{e/\mu}^{\text{loose}} = 2$, $N_{\tau_{\text{had-vis}}}^{\text{loose}} = 0$		$N_{e/\mu}^{\text{loose}} = 1$, $N_{\tau_{\text{had-vis}}}^{\text{loose}} = 1$	$N_{e/\mu}^{\text{loose}} = 0$, $N_{\tau_{\text{had-vis}}}^{\text{loose}} = 2$
e/μ : Medium, gradient iso.		e/μ : Medium, gradient iso.	
		$\tau_{\text{had-vis}}$: Medium	$\tau_{\text{had-vis}}$: Tight
Opposite charge		Opposite charge	Opposite charge
$m_{\tau\tau}^{\text{coll}} > m_Z - 25\,\text{GeV}$		$m_{\text{T}} < 70\,\text{GeV}$	
$30 < m_{\ell\ell} < 75\,\text{GeV}$	$30 < m_{\ell\ell} < 100\,\text{GeV}$		
$E_{\text{T}}^{\text{miss}} > 55\,\text{GeV}$	$E_{\text{T}}^{\text{miss}} > 20\,\text{GeV}$	$E_{\text{T}}^{\text{miss}} > 20\,\text{GeV}$	$E_{\text{T}}^{\text{miss}} > 20\,\text{GeV}$
$E_{\text{T}}^{\text{miss, hard}} > 55\,\text{GeV}$			
$\Delta R_{\tau\tau} < 2.0$		$\Delta R_{\tau\tau} < 2.5$	$0.8 < \Delta R_{\tau\tau} < 2.5$
$\lvert\Delta\eta_{\tau\tau}\rvert < 1.5$		$\lvert\Delta\eta_{\tau\tau}\rvert < 1.5$	$\lvert\Delta\eta_{\tau\tau}\rvert < 1.5$
$0.1 < x_1 < 1.0$		$0.1 < x_1 < 1.4$	$0.1 < x_1 < 1.4$
$0.1 < x_2 < 1.0$		$0.1 < x_2 < 1.2$	$0.1 < x_2 < 1.4$
$p_{\text{T}}^{j_1} > 40\,\text{GeV}$		$p_{\text{T}}^{j_1} > 40\,\text{GeV}$	$p_{\text{T}}^{j_1} > 70\,\text{GeV}, \lvert\eta_{j_1}\rvert < 3.2$
$N_{b\text{-jets}} = 0$		$N_{b\text{-jets}} = 0$	

Signal regions

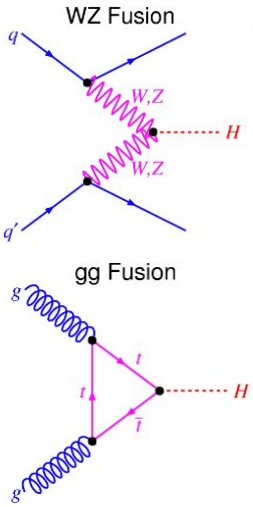

Signal Region		Inclusive	$\tau_{lep}\tau_{lep}$	$\tau_{lep}\tau_{had}$	$\tau_{had}\tau_{had}$
VBF	High-$p_T^{\tau\tau}$	$p_T^{j_2} > 30$ GeV $\lvert\Delta\eta_{jj}\rvert > 3$ $m_{jj} > 400$ GeV $\eta_{j_1} \cdot \eta_{j_2} < 0$ Central leptons	—		$p_T^{\tau\tau} > 140$ GeV $\Delta R_{\tau\tau} < 1.5$
	Tight		$m_{jj} > 800$ GeV	$m_{jj} > 500$ GeV $p_T^{\tau\tau} > 100$ GeV	Not VBF high-p_T $m_{jj} > (1550 - 250 \cdot \Delta\eta_{jj})$ GeV
	Loose		Otherwise		
Boosted	high-$p_T^{\tau\tau}$	Not VBF $p_T^{\tau\tau} > 100$ GeV	$p_T^{\tau\tau} > 140$ GeV $\Delta R_{\tau\tau} < 1.5$		
	Low-$p_T^{\tau\tau}$		Otherwise		

Using pT , ΔR(ττ) and m_{jj}, both inclusive categories are split further into 13 exclusive signal regions with different S/B ratios to improve the sensitivity.

Control regions

Region	Selection
$\tau_{\text{lep}}\tau_{\text{lep}}$ VBF $Z \to \ell\ell$ CR	$\tau_{\text{lep}}\tau_{\text{lep}}$ VBF incl. selection, $80 < m_{\ell\ell} < 100$ GeV (SF)
$\tau_{\text{lep}}\tau_{\text{lep}}$ boosted $Z \to \ell\ell$ CR	$\tau_{\text{lep}}\tau_{\text{lep}}$ boosted incl. selection, $80 < m_{\ell\ell} < 100$ GeV (SF)
$\tau_{\text{lep}}\tau_{\text{lep}}$ VBF top CR	$\tau_{\text{lep}}\tau_{\text{lep}}$ VBF incl. selection, inverted b-jet veto
$\tau_{\text{lep}}\tau_{\text{lep}}$ boosted top CR	$\tau_{\text{lep}}\tau_{\text{lep}}$ boosted incl. selection, inverted b-jet veto
$\tau_{\text{lep}}\tau_{\text{had}}$ VBF top CR	$\tau_{\text{lep}}\tau_{\text{had}}$ VBF incl. selection, inverted b-jet veto, $m_{\text{T}} > 40$ GeV
$\tau_{\text{lep}}\tau_{\text{had}}$ boosted top CR	$\tau_{\text{lep}}\tau_{\text{had}}$ boosted incl. selection, inverted b-jet veto, $m_{\text{T}} > 40$ GeV

Control regions (CRs) used to constrain the Z →ll and top backgrounds to the event yield in data in the lep-lep and lep-had channels.

‘SF’ denotes a selection of same-flavor light leptons.

Normalization factors for backgrounds

Background	Channel	Normalization factors	
		VBF	Boosted
$Z \to \ell\ell$ (CR)	$\tau_{\text{lep}}\tau_{\text{lep}}$	$0.87^{+0.34}_{-0.30}$	$1.25^{+0.29}_{-0.24}$
Top (CR)	$\tau_{\text{lep}}\tau_{\text{lep}}$	1.19 ± 0.09	1.06 ± 0.05
Top (CR)	$\tau_{\text{lep}}\tau_{\text{had}}$	$1.53^{+0.30}_{-0.27}$	1.12 ± 0.07
Fake-$\tau_{\text{had-vis}}$ (data-driven)	$\tau_{\text{had}}\tau_{\text{had}}$	0.88 ± 0.12	
$Z \to \tau\tau$ (fit in each SR)	$\tau_{\text{lep}}\tau_{\text{lep}}, \tau_{\text{lep}}\tau_{\text{had}}, \tau_{\text{had}}\tau_{\text{had}}$	$1.04^{+0.10}_{-0.09}$	1.11 ± 0.05

Normalization factors and their uncertainties obtained from the fit.

The $Z \to \tau\tau$ normalization is constrained by data in the MMC distributions of the signal regions (free floating).

Z → ττ background validation 1/3

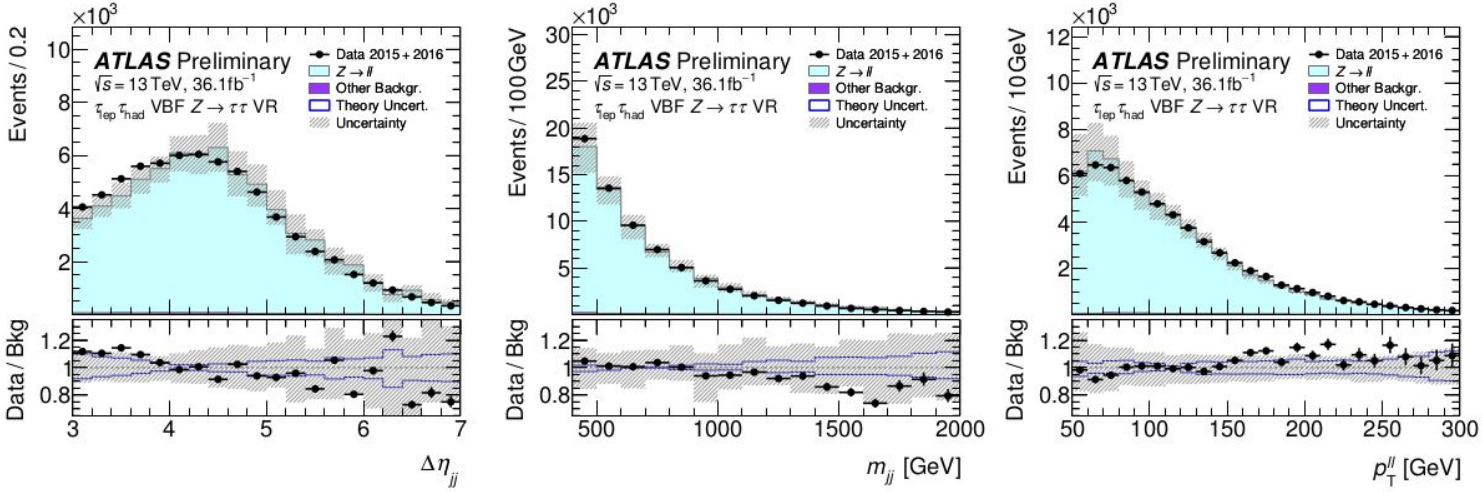

The modeling of the Drell-Yan pp → Z/γ* →ττ background is validated using Z→ττ VRs that consist of Z → ll events.

Z → ττ background validation 2/3

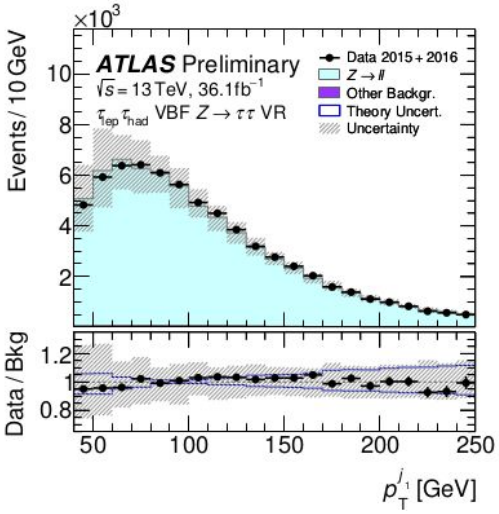

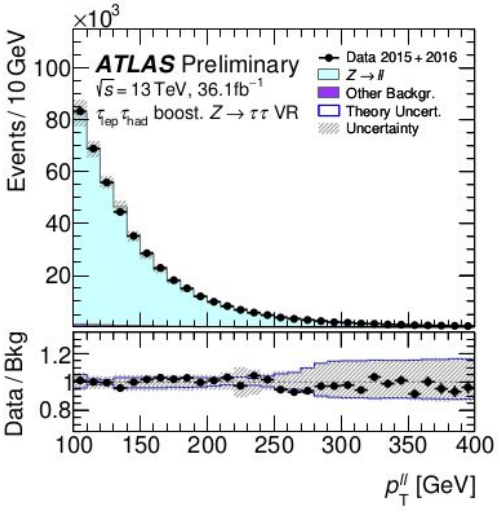

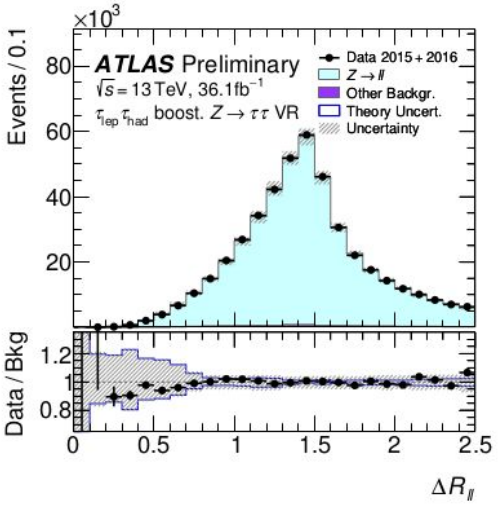

Z → ττ background validation 3/3

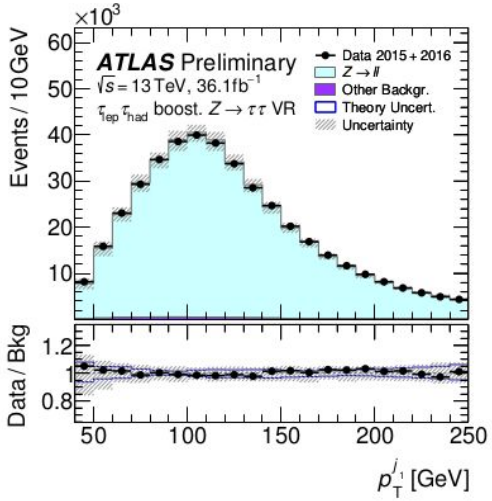

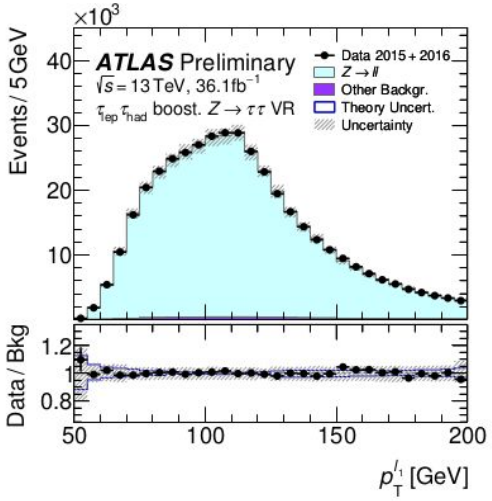

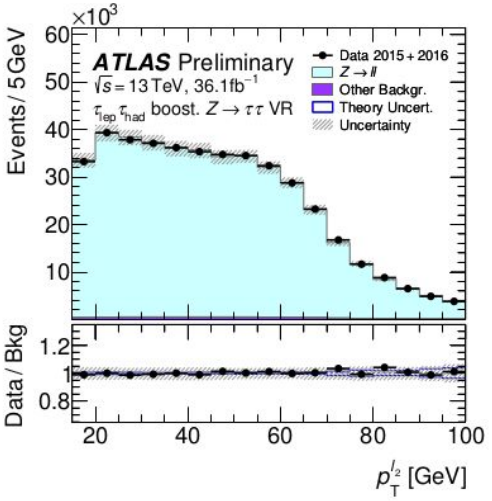

Background Validation

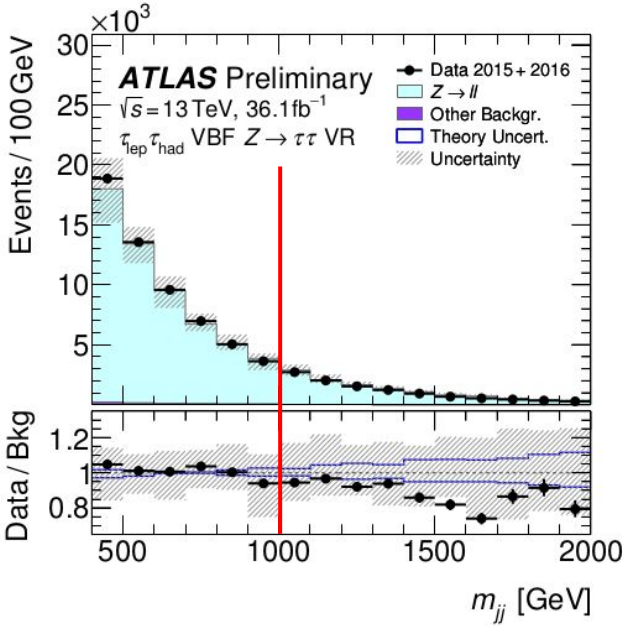

m_{jj} is only used to place categorisation cuts in the range 400-1000 GeV.

The impact of reweighting the MC to the data has been evaluated by using the ratio Data/Bkg and was found that the bias on the significance/μ estimate is negligible.

Results: observed event yields and predictions

	$\tau_{\text{lep}}\tau_{\text{lep}}$ VBF		$\tau_{\text{lep}}\tau_{\text{lep}}$ boosted	
	Loose	Tight	Low-$p_{\text{T}}^{\tau\tau}$	High-$p_{\text{T}}^{\tau\tau}$
$Z \to \tau\tau$	148 ± 14	105 ± 13	2 992 ± 93	2 701 ± 66
$Z \to \ell\ell$	15.8 ± 5.2	20.6 ± 6.7	357 ± 54	235 ± 31
Top	33.3 ± 6.5	25.2 ± 4.6	319 ± 50	188 ± 29
VV	12.0 ± 2.1	10.8 ± 1.5	194.7 ± 8.5	196.2 ± 8.9
Misidentified τ	18.7 ± 9.7	9.8 ± 4.8	212 ± 93	81 ± 35
$ggF, H \to WW^*$	1.2 ± 0.2	1.4 ± 0.3	11.9 ± 2.6	16.4 ± 1.7
VBF, $H \to WW^*$	1.7 ± 0.2	4.1 ± 0.5	2.9 ± 0.3	2.9 ± 0.3
$ggF, H \to \tau\tau$	2.7 ± 1.0	2.0 ± 1.0	33.5 ± 8.9	33.0 ± 9.3
VBF, $H \to \tau\tau$	5.2 ± 1.5	11.4 ± 3.1	7.6 ± 2.1	8.2 ± 2.3
$WH, H \to \tau\tau$	< 0.1	< 0.1	2.4 ± 0.7	3.1 ± 0.9
$ZH, H \to \tau\tau$	< 0.1	< 0.1	1.3 ± 0.4	1.6 ± 0.5
Total background	231 ± 14	177 ± 12	4 089 ± 65	3 420 ± 57
Total signal	8.1 ± 2.3	13.5 ± 3.7	46 ± 12	47 ± 12
Data	237	188	4124	3444

Fitted signal and background yields expected in each signal region.

Errors include statistical and systematic uncertainties.

Results: observed event yields and predictions

	$\tau_{\text{lep}}\tau_{\text{had}}$ VBF		$\tau_{\text{lep}}\tau_{\text{had}}$ boosted	
	Loose	Tight	Low-$p_{\text{T}}^{\tau\tau}$	High-$p_{\text{T}}^{\tau\tau}$
$Z \to \tau\tau$	175 ± 18	319 ± 22	4 159 ± 96	5 313 ± 92
$Z \to \ell\ell$	10.1 ± 3.0	12.6 ± 3.0	130 ± 37	115 ± 16
Top	5.8 ± 1.6	17.9 ± 4.7	119 ± 20	56 ± 10
Misidentified τ	103 ± 16	100 ± 15	1 907 ± 77	617 ± 27
Other backgrounds	4.0 ± 1.6	9.5 ± 1.9	115.2 ± 7.9	129.6 ± 8.9
$ggF, H \to \tau\tau$	4.1 ± 1.3	7.0 ± 2.0	62 ± 16	64 ± 21
VBF, $H \to \tau\tau$	7.5 ± 2.2	25.3 ± 7.1	12.0 ± 3.5	14.2 ± 4.1
$WH, H \to \tau\tau$	< 0.1	0.1 ± 0.0	4.0 ± 1.1	5.3 ± 1.4
$ZH, H \to \tau\tau$	< 0.1	< 0.1	1.8 ± 0.5	2.8 ± 0.8
Total background	299 ± 18	459 ± 23	6 430 ± 88	6 230 ± 92
Total signal	11.7 ± 3.3	32.5 ± 8.4	80 ± 20	86 ± 24
Data	318	496	6556	6347

Results: observed event yields and predictions

	$\tau_{had}\tau_{had}$ VBF			$\tau_{had}\tau_{had}$ boosted	
	Loose	Tight	High-$p_T^{\tau\tau}$	Low-$p_T^{\tau\tau}$	High-$p_T^{\tau\tau}$
$Z \to \tau\tau$	69.0 ± 9.5	103 ± 12	144 ± 12	3 260 ± 130	3 592 ± 85
Misidentified τ	45.1 ± 5.4	96.4 ± 9.2	19.8 ± 2.9	1 870 ± 140	366 ± 54
Other backgrounds	4.4 ± 1.4	11.5 ± 1.7	4.4 ± 0.7	281 ± 21	109.9 ± 9.2
$ggF, H \to \tau\tau$	1.1 ± 0.4	2.0 ± 0.7	3.5 ± 1.1	41 ± 11	49 ± 15
VBF, $H \to \tau\tau$	1.5 ± 0.5	6.4 ± 1.8	11.0 ± 3.0	8.9 ± 3.4	10.6 ± 2.9
$WH, H \to \tau\tau$	< 0.1	< 0.1	< 0.1	3.3 ± 1.0	4.4 ± 1.2
$ZH, H \to \tau\tau$	< 0.1	< 0.1	< 0.1	2.4 ± 0.7	2.8 ± 0.8
Total background	119 ± 10	210 ± 13	168 ± 13	5 411 ± 80	4 068 ± 66
Total signal	2.6 ± 0.8	8.4 ± 2.4	14.6 ± 3.8	56 ± 15	67 ± 18
Data	121	220	179	5455	4103

Observed and expected m_{TT} distributions - VBF

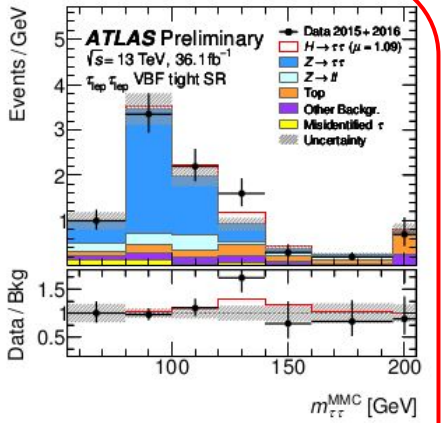

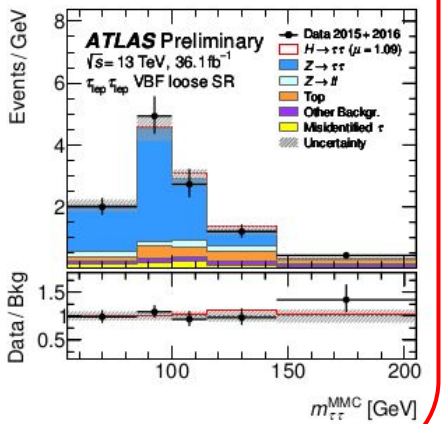

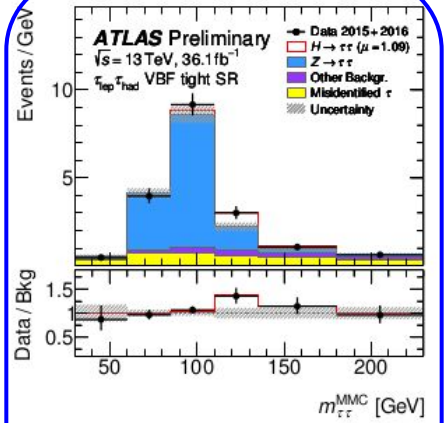

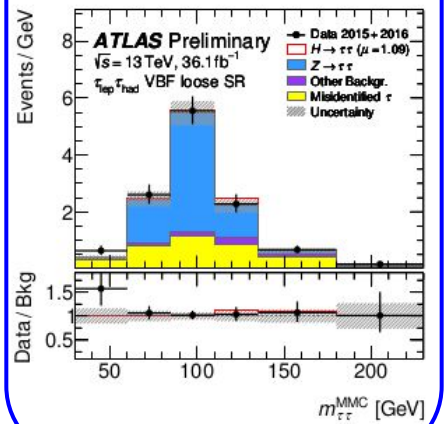

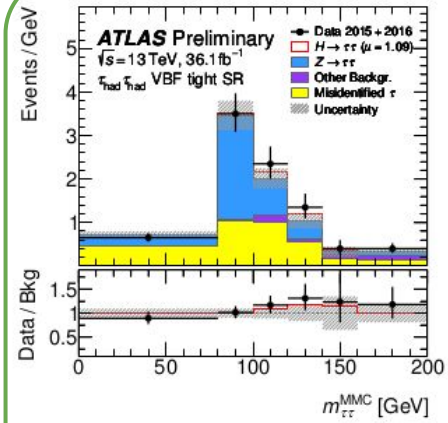

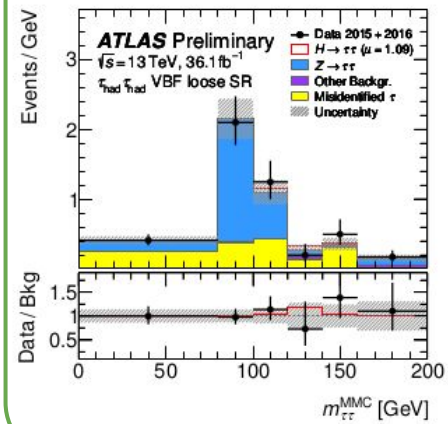

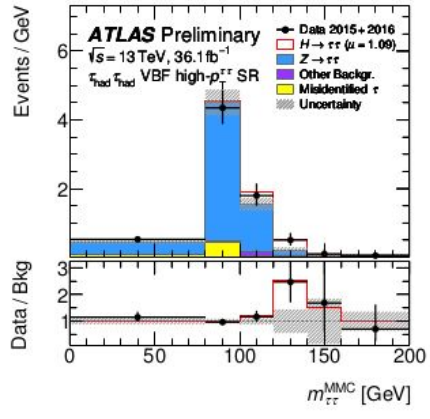

Observed and expected m_{TT} distributions - Boosted

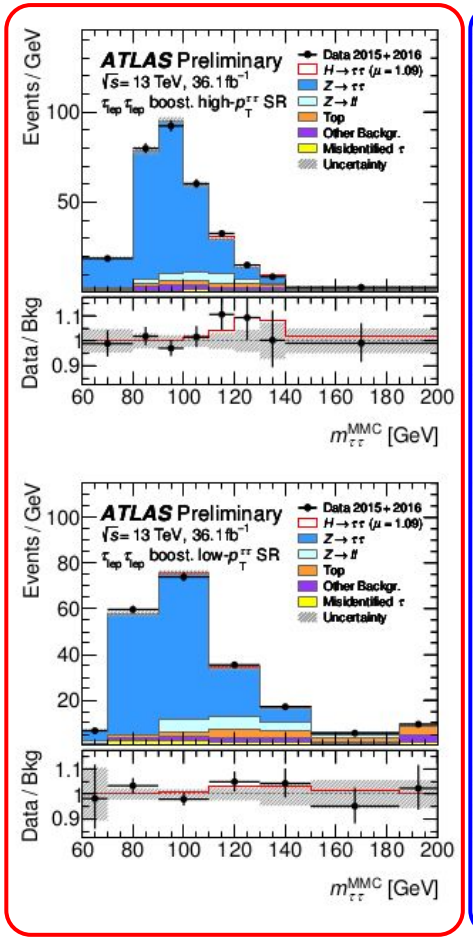

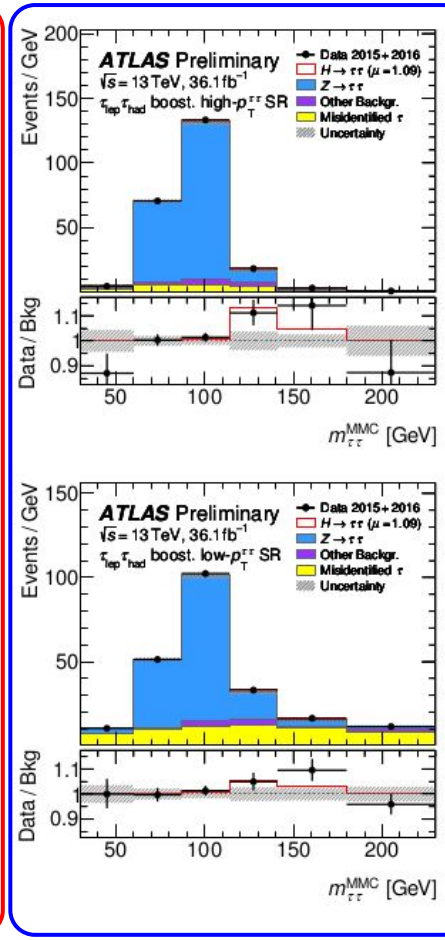

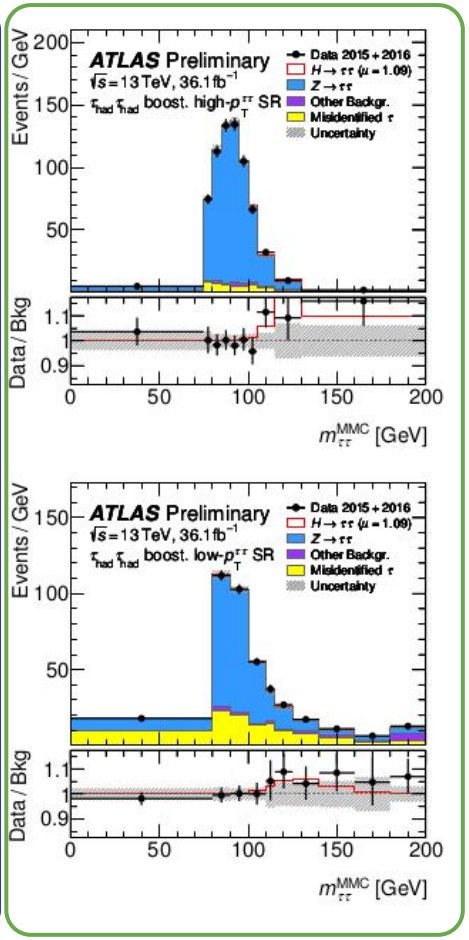

Theoretical uncertainties in signal - ggF (9 sources)

Production σ(ggF) in association with an exclusive number of additional jets has large uncertainties from higher-order QCD corrections:

1. Two sources account for yield uncertainties due to factorization (μ_F) and renormalization (μ_R) scale variations
2. Two sources account for migration uncertainties of $N_{jets}=0$ to $N_{jets}=1$ and $N_{jets}=1$ to $N_{jets}\geq 2$ in the event using the STWZ and BLPTW predictions as an input

Higgs boson-pT (dominant in all SRs):

1. Two sources encapsulate the migration uncertainty between the intermediate and high-pT regions of events with $N_{jets}\geq 1$
2. One encapsulates the uncertainty in the loop corrections due to the top-quark mass uncertainty, where the difference between the LO and NLO predictions is taken as an uncertainty due to missing higher-order corrections.

Acceptance:

1. Two sources account for the acceptance uncertainties of ggF production in the VBF phase space from selecting exactly two and at least three jets, respectively.

→ The resulting acceptance uncertainties from these nine sources range from 1-10%.

Theoretical uncertainties in signal

Underlying event, hadronization and parton shower uncertainties for all signal samples are estimated by comparing the acceptance when using the default UEPS model from Pythia 8.212 with an alternative UEPS model from Herwig 7.0.3.

→ The resulting acceptance uncertainties range from 2–26% for ggF production and from 2–18% for VBF production.

PDF uncertainties are estimated using 30 eigenvector variations and two α_s variations that are evaluated independently with respect to the default PDF set PDF4LHC15.

→ Total uncertainty is 5% or less depending on the SR and the Higgs production mode.

Uncertainty in the H → ττ decay branching ratio of 1% affects the signal rates.

→ The resulting acceptance uncertainties from these nine sources range from 1-10%.

Interpretation to JER/JES systematics

Uncertainties related to jet energy resolution and scale have fitted parameters which are shifted with respect to the nominal value.

The $m_{\tau\tau}$ reconstructed from real di-tau events is sensitive to JES/JER.

Selected di-τ events in VBF and boosted categories are characterized by one or more high-pT jets which recoil against the two τ leptons.

The main contributions to MET are thus the neutrinos in the τ lepton decays and the impact of the jet energy resolution when projected onto the MET direction.

Applying both JER and JES uncertainties causes a shift in the mean jet pT, which therefore translates directly into a shift of the reconstructed MET.

This, in turn, translates into a shift of the reconstructed MMC di-τ mass that is constrained by data in the $Z \rightarrow \tau\tau$ mass peak.